SOFT LANDER PLATFORM

Contributed instrumentation

(Astrobiology Wet Laboratory)

J. Gómez-Elvira, J. Lasue, O. Prieto

IRAP, Toulouse

September 6-9, 2016

Lake Bonney, McMurdo Dry Valleys of Victoria Land, **Antarctica**.

GOAL

We propose to complement the lander objectives in three specific points using additional surface platforms lead by ESA:

1. Understand the exchange processes between the aqueous interior environments and the surface, focusing on the hydrochemistry and physical state of the ice crust.
2. Search for evidence of life on Europa.
3. Characterize the biosignature preservation potential (BPP) of accessible surface materials at the landing site.

For 1 and 2 objectives of AWL are in agreement with the NASA lander driven philosophy, our analytical approach is different, **since EI instruments consider liquid samples rather than solid one**.
For third objective, the propose is a radiation measurement.

In addition to them, some other requirements are identified:

- Investigate areas **away from the influence of the landing manoeuvres** e.g., by the sky-crane, preferentially more protected from radiation at local scale (TBD).
- Avoid the surface altered compounds, so **sample the subsurface.**

(from Science Case doc.)

GOAL

TRACEABILITY MATRIX

Investigation	Measurement	Requirement	Instrument
Characterize the hydrochemistry of endogenic fluids	Physical chemistry: Acidity, redox, conductivity and temperature of samples in liquid state	pH (to 1 unit) redox (TBC) conductivity (TBC) temperature (0.1 K)	Multiparametric electrode sensor
	Volatiles in ice (augmented capability if AWL)	O2, CH4 (TBC)	Multiparametric electrode sensor

Goal	**Investigation**	**Requirement**	**Instrument**
Search for evidence of life on Europa	Detect potential biomolecules	Identify biomolecules such as: D/L aromatic aa PAHs Short peptides Anti-freezing peptides and sugars EPS from psychrophilic microbes Cold shock proteins (Concentration <10ppb)	Multiarray immunoassay detector

(from Science Case doc.)

SCIENCE REQUIREMENTS

1. Liquid sample of subsurface away from the influence of landing manoeuvres.
2. Measurements (TBC):
    1. pH (resolution 1 unit)
    2. Potential redox
    3. Conductivity
    4. Temperature (resolution 0.1K)
    5. Dissolved gases: O_2 , CH_4
    6. Radiation: electrons, ions (K^+, Na^+, -TBC)
    7. Magnetic field
    8. Organic molecules with concentration < 10 ppb (TBC) :
        1. D/L aromatic aa
        2. PAHs
        3. Short peptides
        4. Antifreezing peptides and sugars
        5. Exopolisacarides
        6. Cold shock proteins

ENVIRONMET

1. Surface Temperature: 100 K
2. Sun radiation: TBD
3. Jupiter radiation: see next page
4. Pressure: 10^{-11} bars
5. Particles radiation: TBD

ENVIRONMET

RADIATION

Landing site candidates

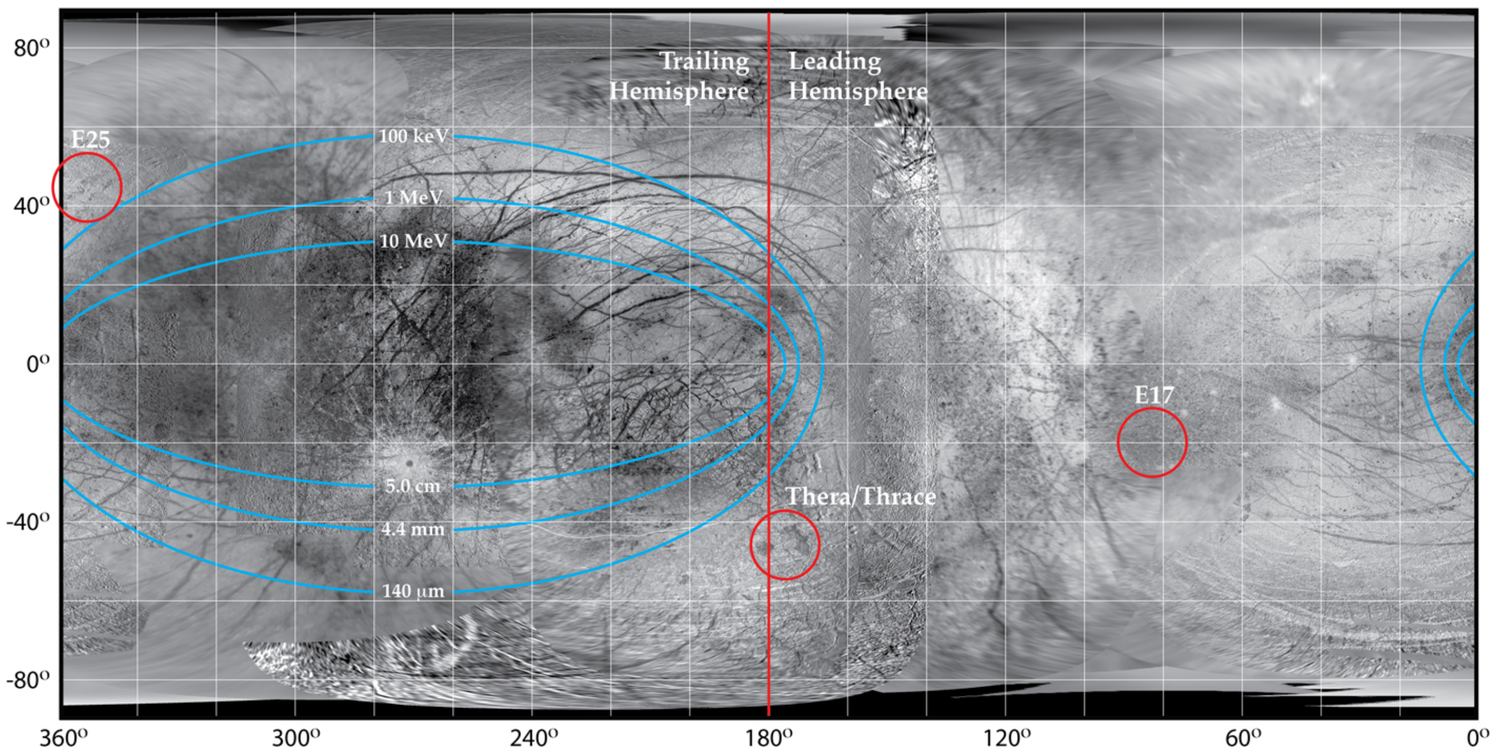

Source: L.Prockter. Europa lander Study, 2012

Landing distance from lander

NASA has not release information about the landing concept. Nevertheless, in the past two options were used: Phoenix, inherited from Viking, concept based on last seconds descends controlled by thrusters., or MSL which implemented the sky crane concept to minimize the soil degradation. In both cases the zone close to the landing was altered by the thrusters (see images).

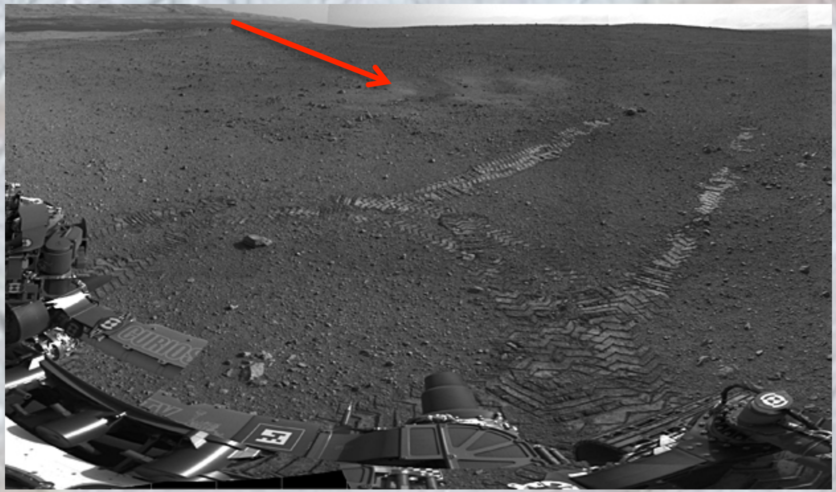

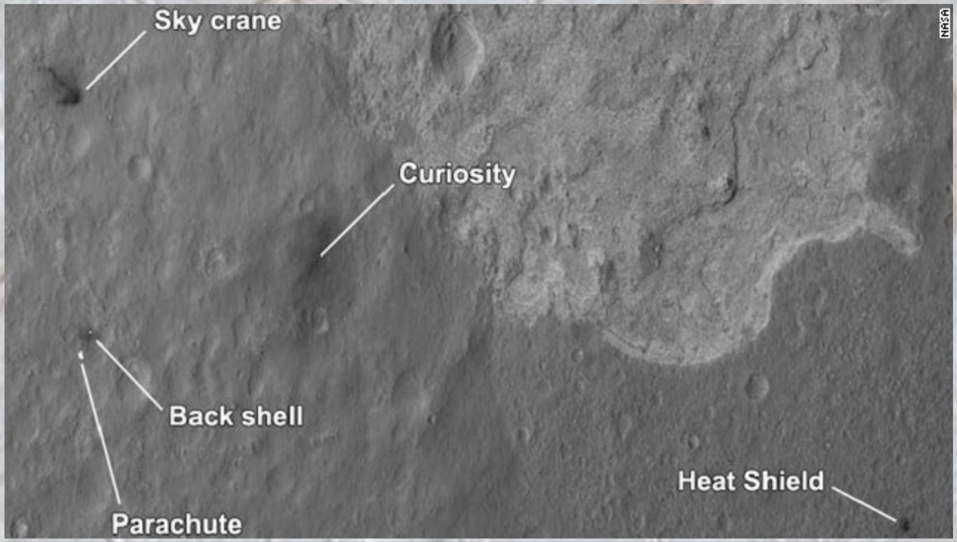

Images of Curiosity landing site where is possible to see the erosion effect of sky-crane thrusters,

ENVIRONMENT

SURFACE MORPHOLOGY

Earth images

Source: L.Prockter. Europa lander Study, 2012

No enough image resolution of Europa surface, but we could expect extremely rough terrain

B. Goldstein, R. Pappalardo. OPAG, March 30, 2016

K. Hand, A. Murray, J. Garvin. OPAG August 11, 2016

NASA LANDER CONCEPT

Top-Level Mission Event Sequence

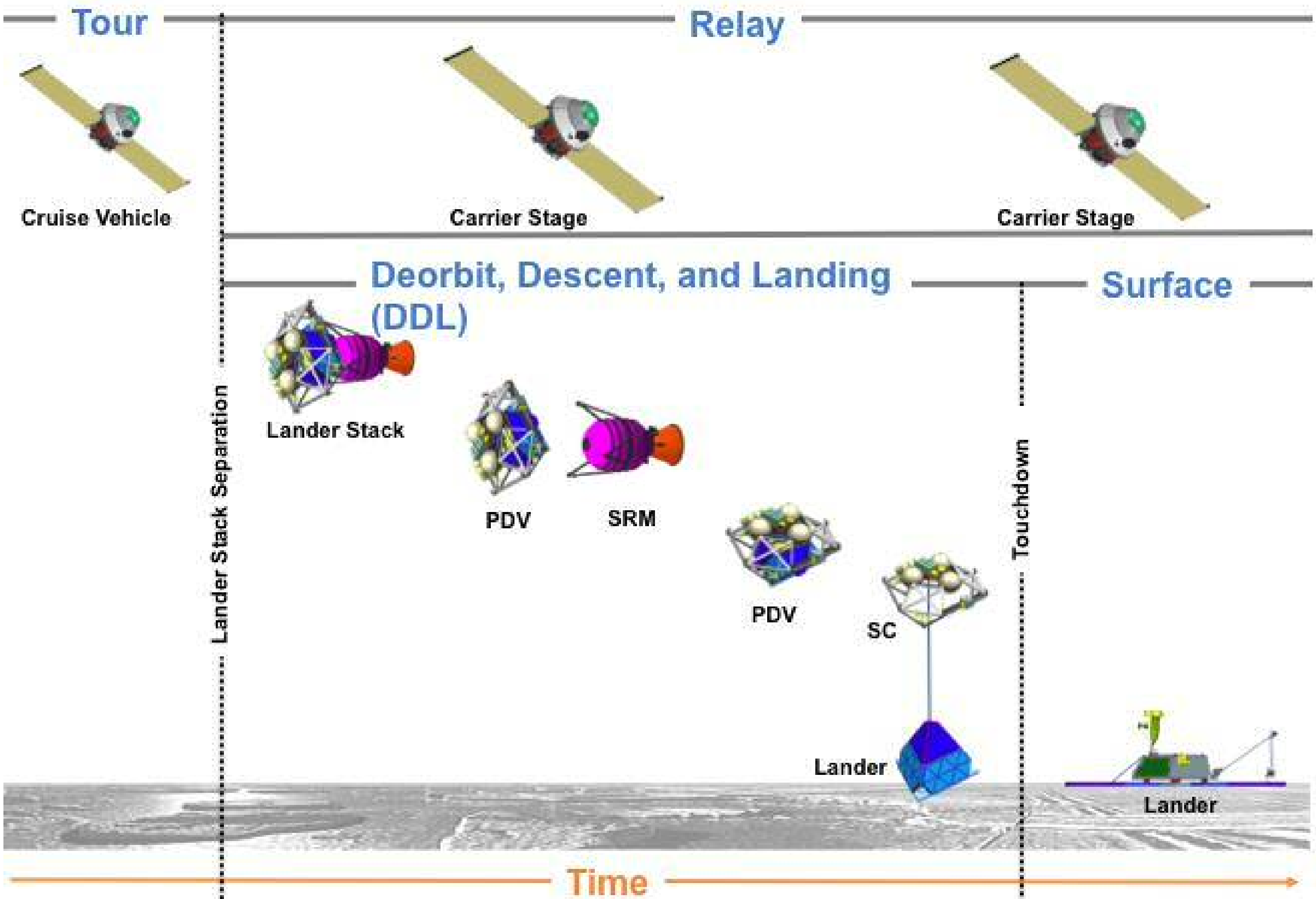

(Image source: JonLomberg.com Giclee Prints)

Model Payload (Total Mass: 25 kg MEV)

- Centerpiece Instruments for Astrobiology
  - **GCMS**: VCAM GC + Ion Trap MS, 8.3 kg CBE
  - **Raman**: SHERLOC 5.4 kg CBE

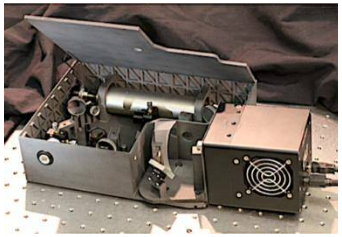

- Auxiliary Instruments
  - **Context LanderCams (x2)**, 0.5 kg each CBE
  - **Microscopic SampleCam**, 0.5 kg CBE

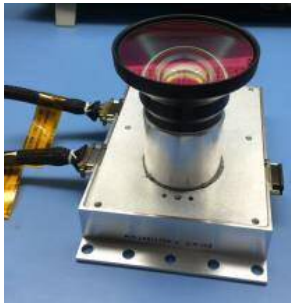

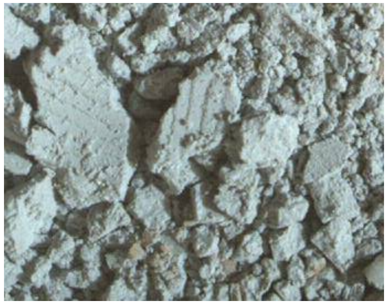

- Baseline Instrument (not included in Threshold)
  - **3-axis Geophone**, 0.8 kg

Payload Envelopes

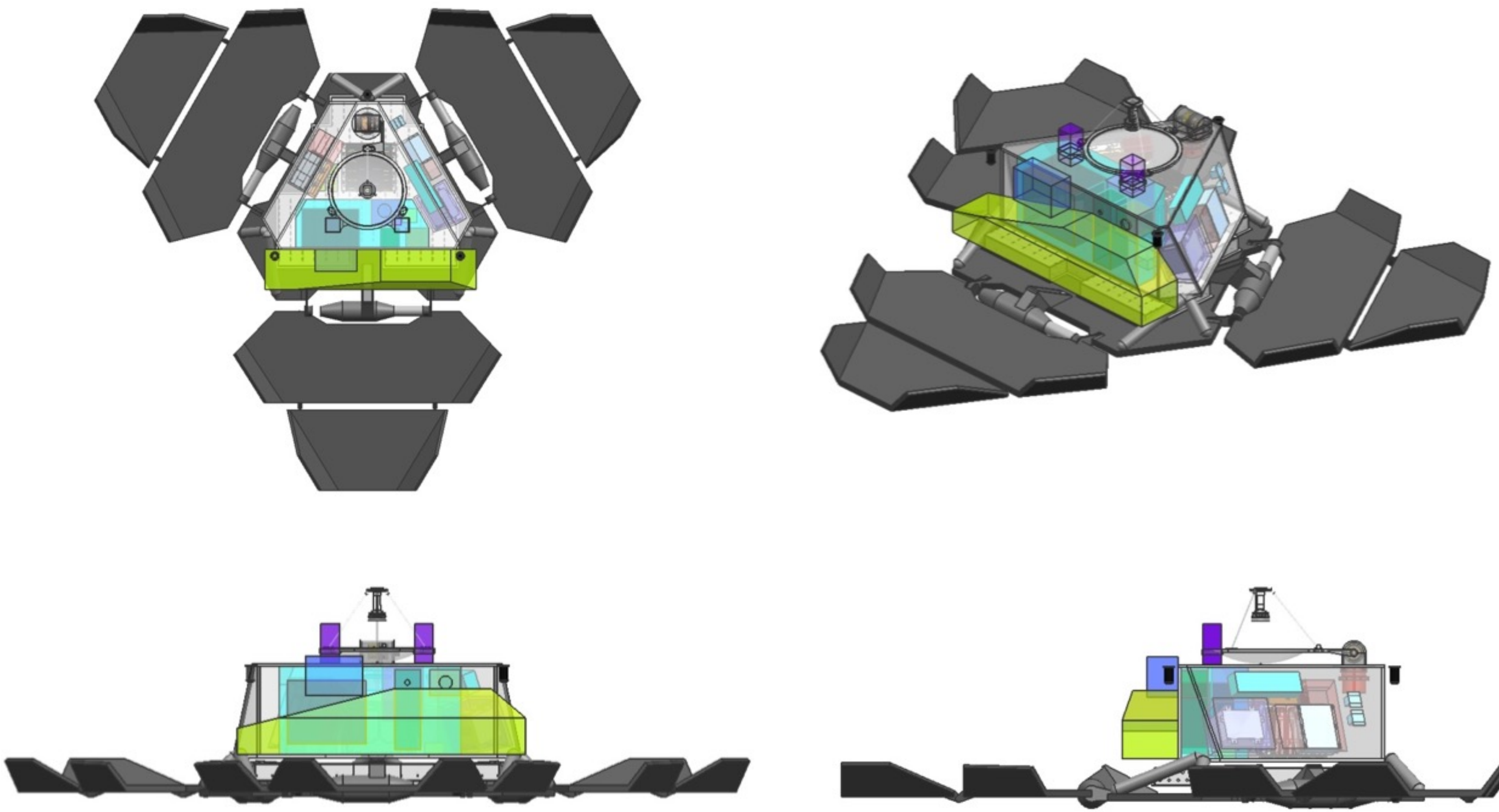

Europa Lander. Science Definition Team Update. OPAG August 11,2016. K. Hand et al.

Lander in Sampling Configuration

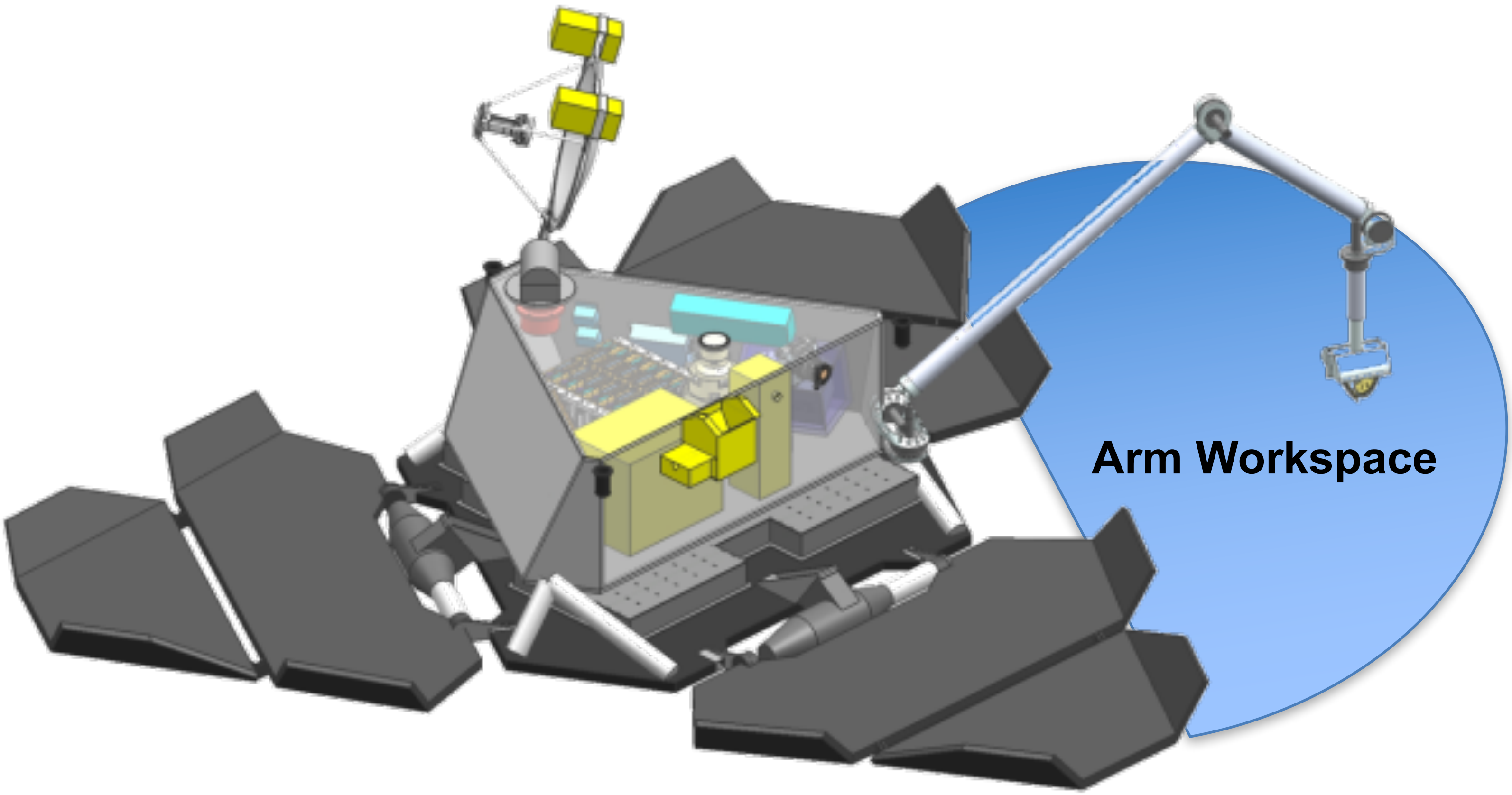

Europa Lander. Science Definition Team Update. OPAG August 11,2016. K. Hand et al.

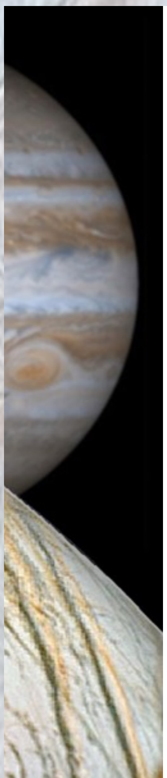

Payload Resource Allocations

	Mass (kg)	Current Volume (cm3) (MEV)	Total Energy per Mission* (W-hr) (CBE)	Total Data Volume per Mission* (Mbits) (CBE)
Europa Lander Payload	35.0 kg (26.6 kg with 32% margin)	24900 cm3	2500	2700

Europa Lander. Science Definition Team Update. OPAG August 11,2016. K. Hand et al.

Concepts for Ocean worlds Life Detection Technology
NASA AO NNH16ZDA001N-CLDTCH Released on Feb. 19, due date June 17.

The current Europa lander mission concept envisions a "soft" landing system that would deliver the lander with a total mass of approximately 300 kg to the surface. The mission concept is anticipated to have a surface lifetime of less than 30 days using a power system consisting of solar panels and/or batteries. The lander would provide the ability to deliver multiple surface and/or subsurface samples to instruments. The anticipated prioritized goals of this mission are [SDT charter mission goals] :
1. Search for evidence of biomarkers and/or life, especially extant life.
2. Assess the habitability (particularly through quantitative compositional measurements) of Europa via in situ techniques uniquely available to a landed mission.
3. Characterize surface properties at the scale of the lander to support future exploration, including the local geologic context.
The payload for this mission is not yet specified, but the payload and its resource allocation are expected to be quite limited due to the challenges posed by landing on Europa. While still under study, the current best estimates (CBE) for resource allocations for the entire payload are:
• 35 kg (26.6 kg CBE with 32% margin)
• 24,900 cm3 (maximum expected value)
• 2,500 W-hrs (CBE for entire surface mission) • 2,700 Mbits (CBE for entire surface mission)

DESIGN

Preliminary list of design drivers and assumptions:

1. **AWL is ejected from the lander and lands (soft impact) at 50 m (TBC).**
2. **Mission duration 2 days (TBC)**
3. **Liquid sampling subsurface 5 cm(TBC)**
4. **Instrumentation ** From science requirements**
5. **Environment ** No data NASA lander data available**
6. **Budgets (mass, power, dimensions) restrictions ** No data NASA Lander data available**
7. **Communications restrictions ** No data NASA lander data available**

MECHANICAL CONCEPT

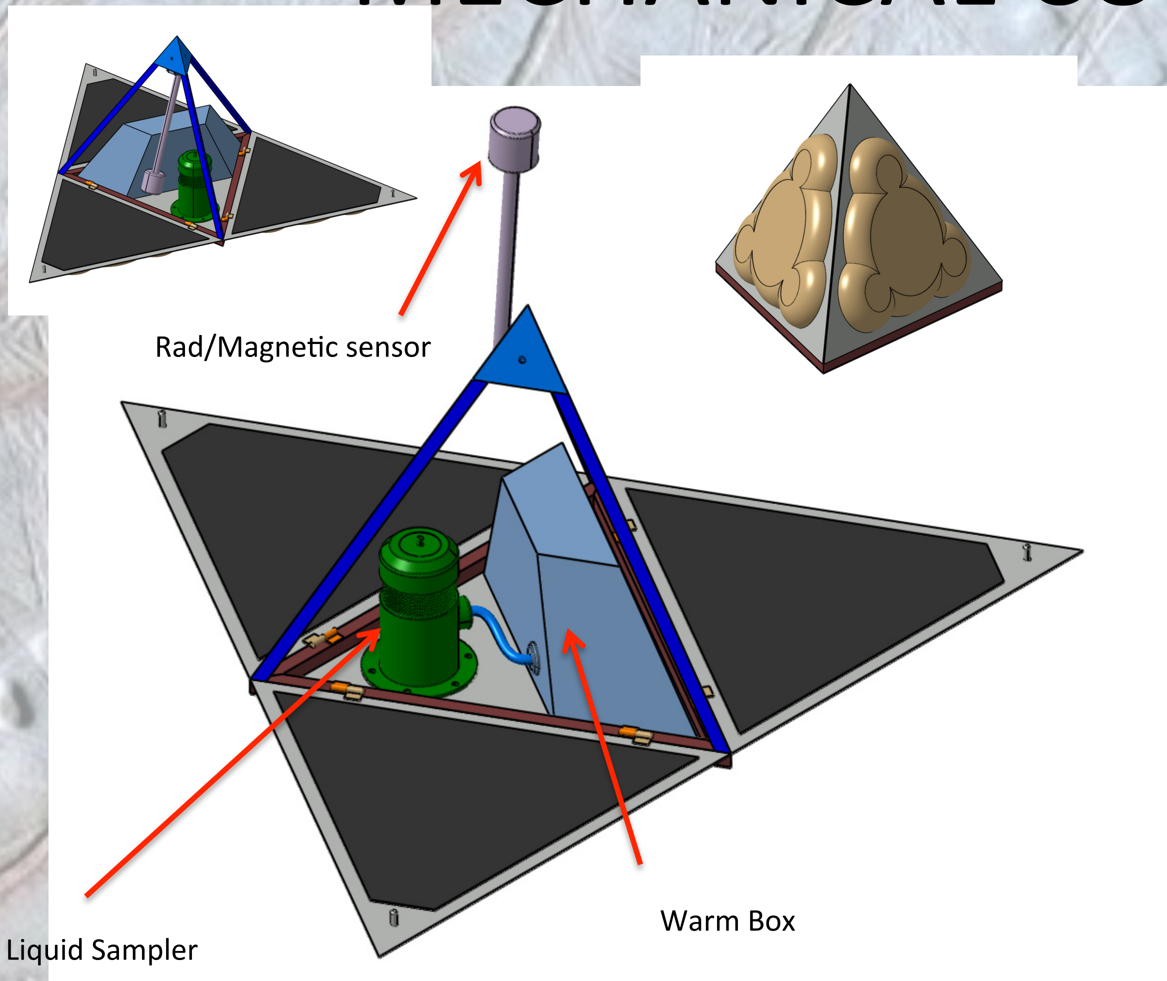

AWL DESIGN CONCEPT

- Similar **concept followed in Mars Pathfinder**. A tetrahedron whit three sides deployable which allows to get vertical orientation knowing the gravity vector direction after landing.
- A **deployable boom** to isolate the magnetometer from the AWL body (similar to Rosetta concept).
- A **warm box** for electronics, batteries and chemical instrumentation. Also for protecting from radiation.
- Some protection is foreseen in the lateral face of the tetrahedron to mitigate the impact, even some mini-airbags could be implemented. (*)
- The **ejection** from the lander will controlled by a spring and a HDRM. (*Alternative InSight concept*)

(* ESA qualified design)

BLOCK DIAGRAM

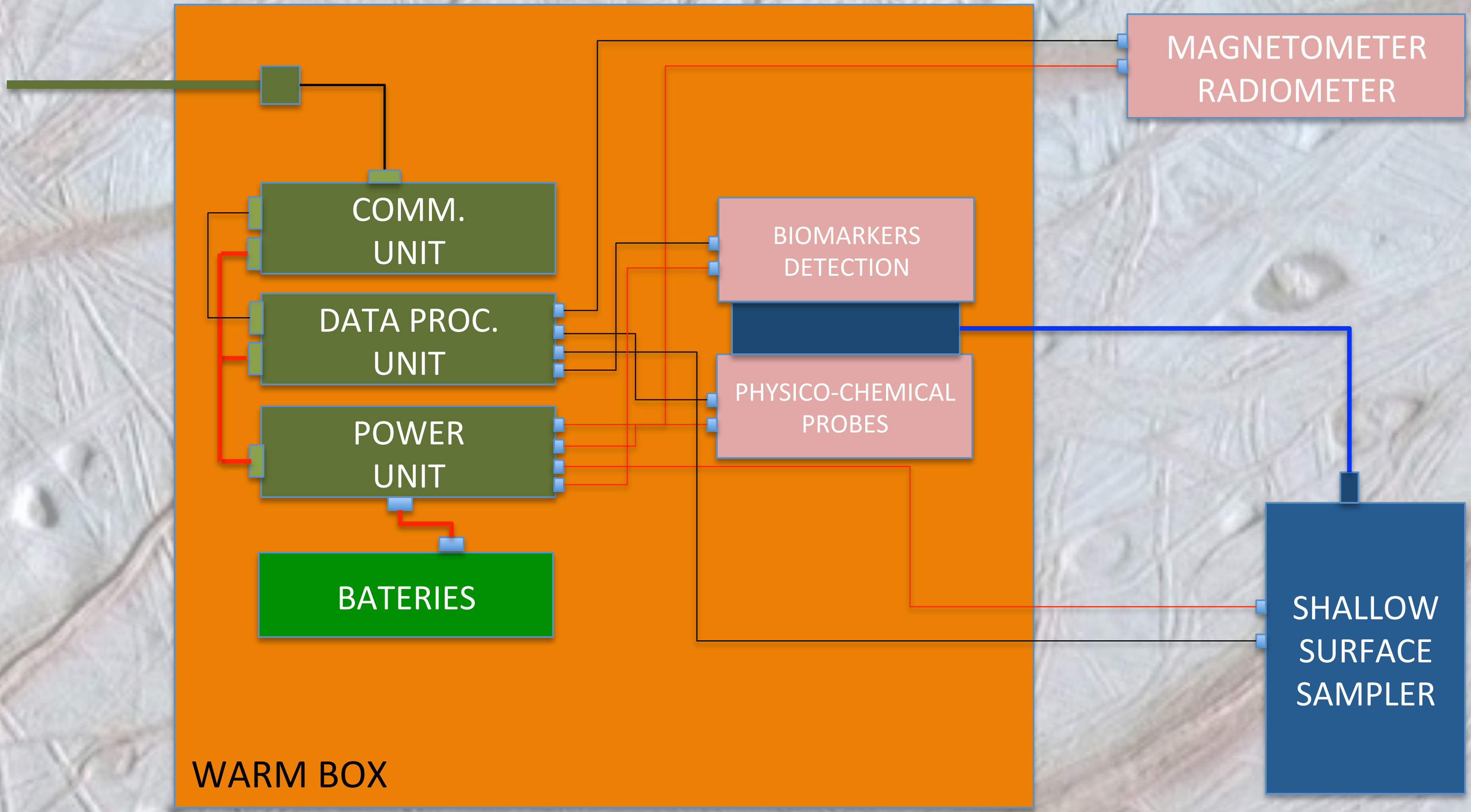

SAMPLING CONCEPT (I)

The concept proposed is a thermal drill based with a laser as source of drilling energy. A diode laser infrared (10.6 to 1.064 µm [1]) with a power of 10 watts. With the laser is possible to remove the first 5cm of surface.

Step 1. At some distance makes a hole up to 5 cm deep

Step 2. The drill head in contact with the ice activated the laser and make a hole of around 1cm deep. Keeping a core insight.

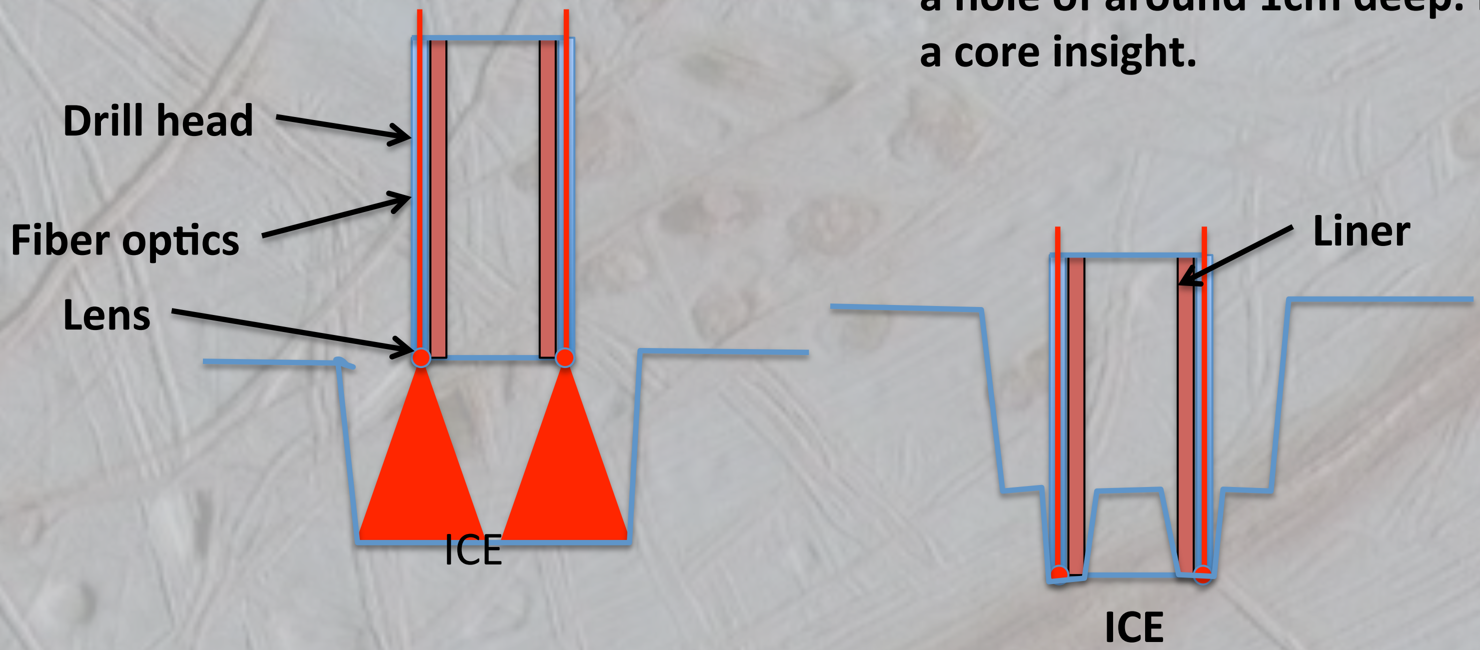

[1]Sakurai et al, Studies of melting ice using CO2 laser for ice drilling. Cold Regions Science and Technology (2011)

SAMPLING CONCEPT (II)

- Step 3. Internal liner is pressurized up to 5 – 10 kPa (0.05 to 0.1 bar) .
- Step 4. The liner is heated until all the core is liquefied.
- Step 5. A syringe absorbs all the fluid to warm box to a deposit where at the inlet for physic-chemical properties and the organic molecule detection.

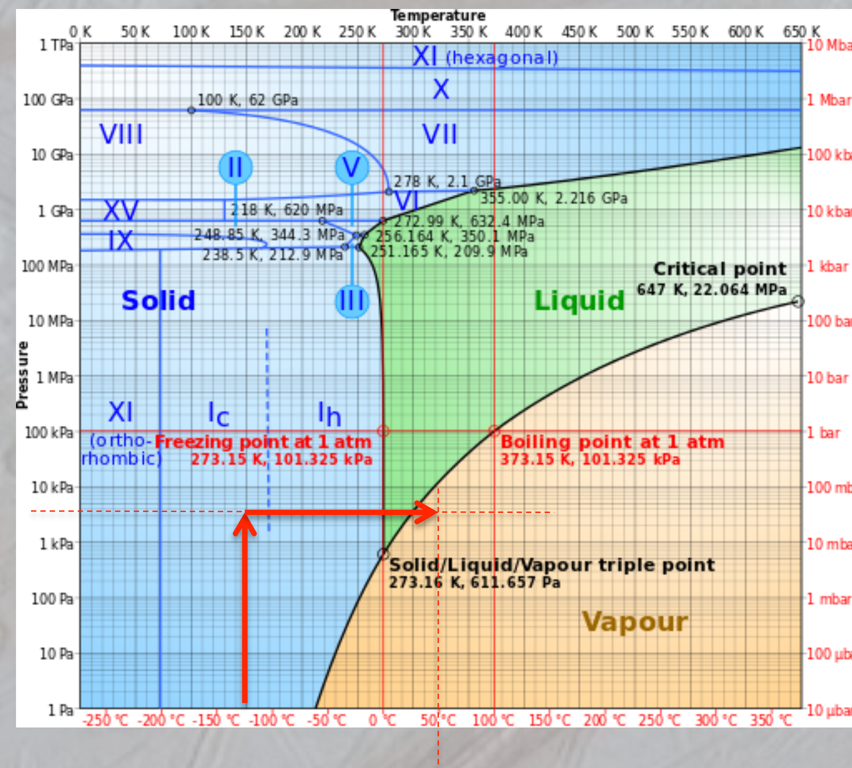

Planetary protection: esterilized and free of organic material. Some protection for isolation during operation on Earth.

SAMPLING CONCEPT (III)

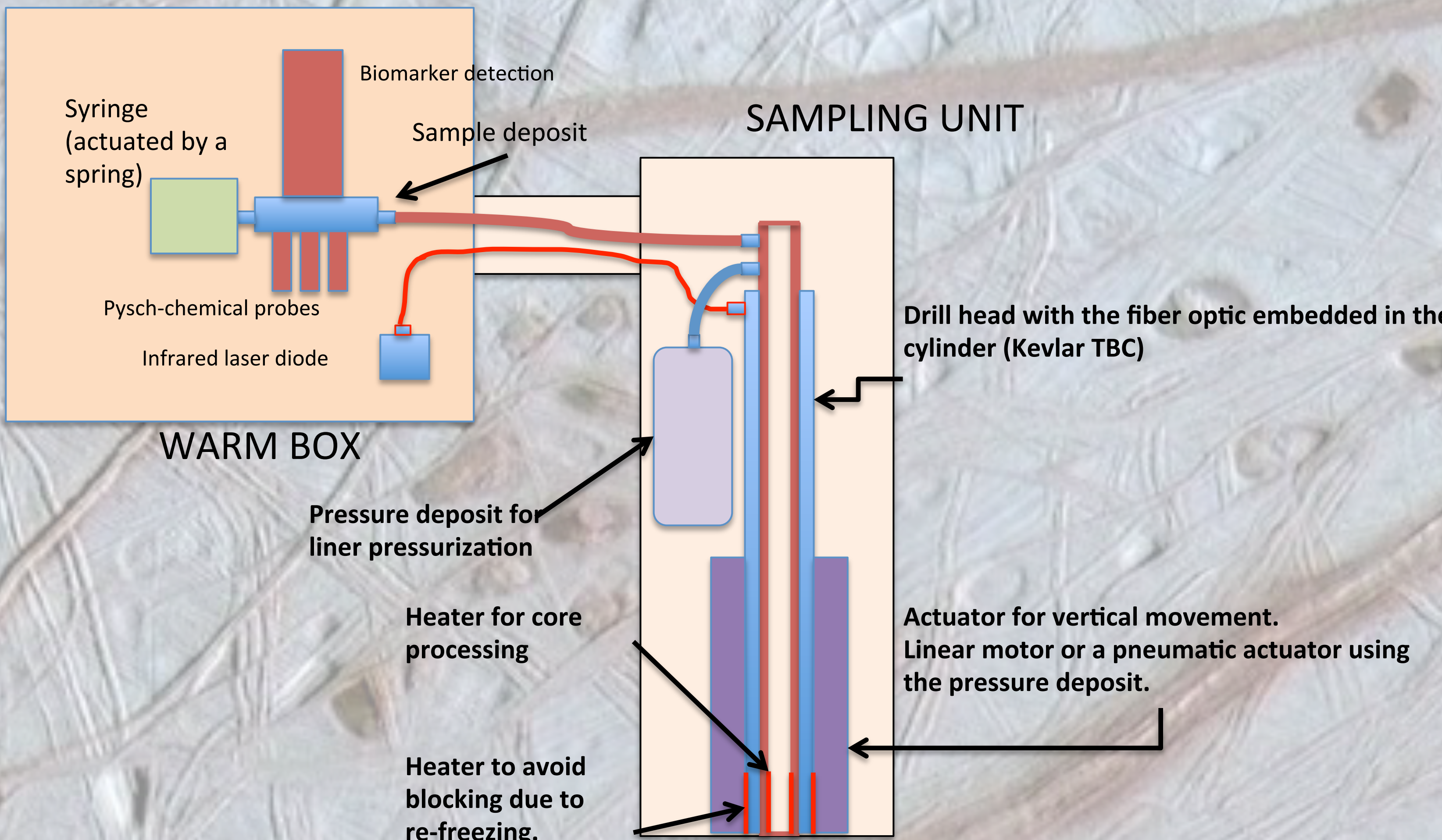

Power estimated 10 watts for 1 hour of drilling TBC. (with pneumatic actuator).

MAGNETOMETER

Based on ROMAP

TABLE II

ROMAP resources requirements

Resources	Experiment part	Requirements	∑
Mass	MAG sensor	40 g	
	SPM sensor	120 g	
	Pressure sensor	110 g	
	Boom + hinge + cable	80 g	
	Launch lock	40 g	
	Pressure harness	50 g	
	Electronics in CEB (interface, analogue, controller, HV-box, connectors, frontplate)	360 g	
	Pressure E-Box	130 g	930 g
Power	Ssensor electronics	350...550 mW	
	Controller	180 mW	
	Penning electronics	100 mW	
	Pirani electronics	50 mW	
	HV-part	200 mW	<900 mW
Telemetry rate	surface mode		
	MAG	70 bits/s	
	SPM	30 bits/s	80 bits/s
	Slow mode		
	MAG	70 bits/s	68 bits/s
	Fast mode		
	MAG	4400 bits/s	4369 bits/s

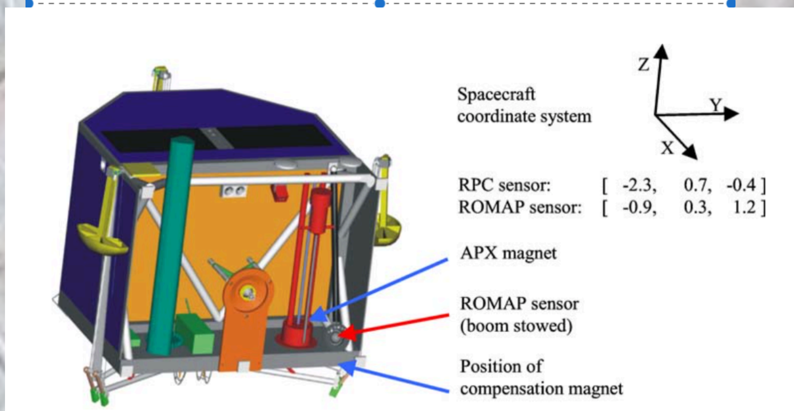

Figure 10. Accommodation of ROMAP sensor and main DC disturbance sources (distances in m with respect to spacecraft reference point).

ROMAP ROSETTA lander requirements

Range ±2000 nT
Quantization 10 pT
Sensor noise: < 5 pT/sqrt(hz) at 1 Hz
Freq. Range 0 .. 32 Hz
Ions 40 ... 8000eV, resoution 7%
Electron 0.35 ... 4200 eV, resolution 15%

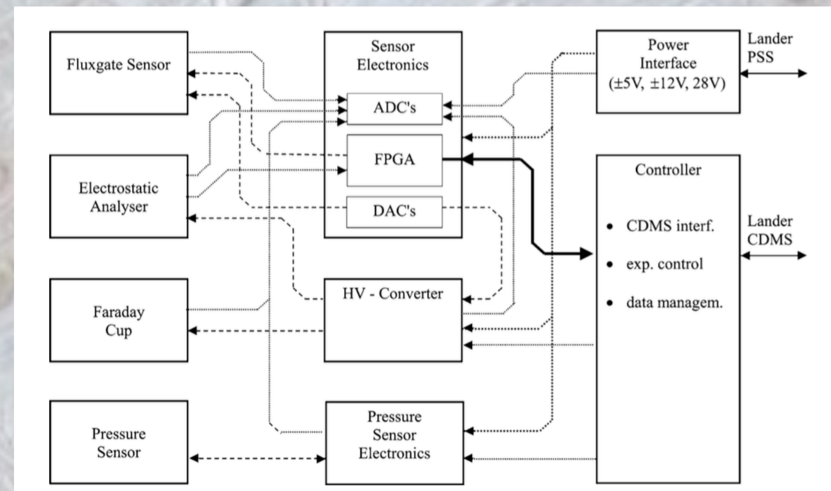

Figure 7. ROMAP block diagram.

Ref.: Auster et al. ROMAP: Rosetta Magnetometer and Plasma Monitor . SSR(2007)128

PHYSICO CHEMICAL PARAMETERS DETECTION

Due to the resources restriction, the concept should be based on reliability and miniaturization. The Phoenix wet lab instrumentation is to large.
The proposed concept is based on ISFET or CHEMFET detectors[1] based on environmental monitoring on earth.

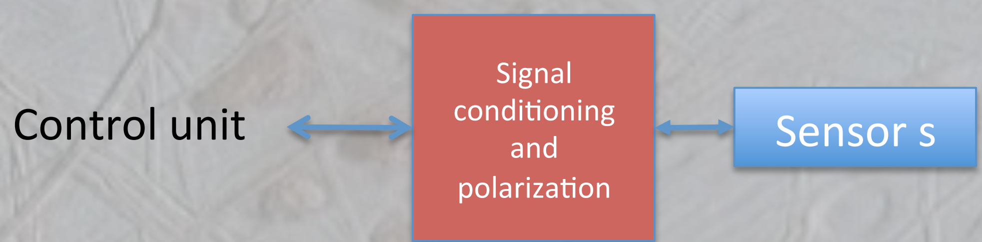

Power consumption is the range of miliwatts and mass in the order of grams.

[1] Jimenez-Jorquera C. et al, ISFET Based Microsensors for Environmental Monitoring. Sensor (2010) 10.

BIOMARKER DETECTION

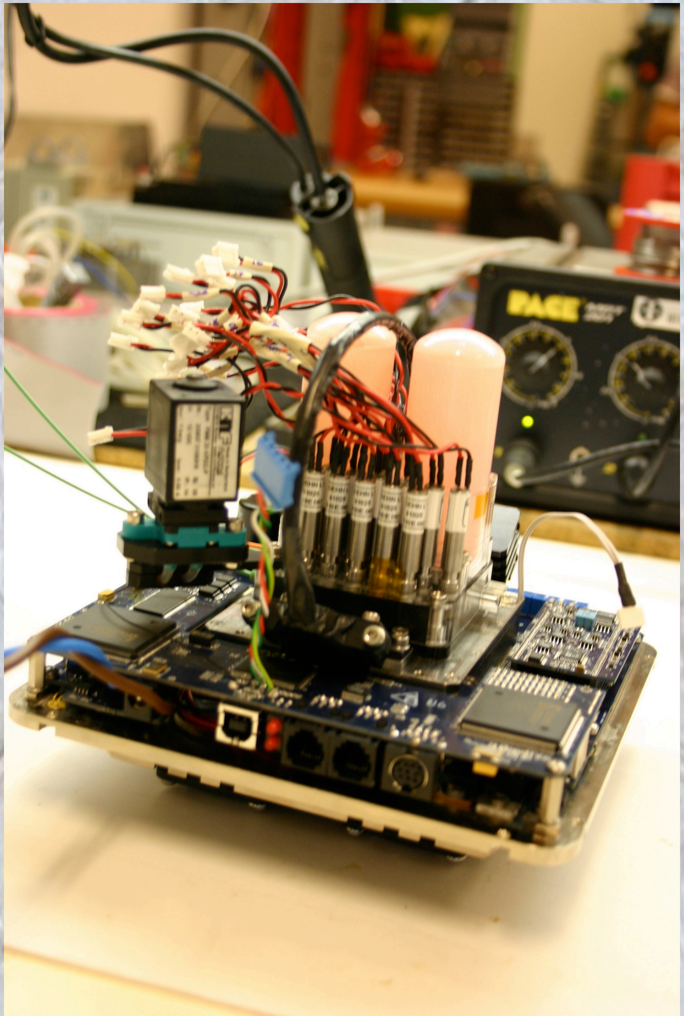

Credit: Centro de Astrobiología (CSIC-INTA)

CAB has experience in developing molecular biomarker detection system based on immunoassay tests. It has a library of more than 400 antibodies. Some of them tested against radiation (Mars levels).

The proposal for AWL is to give a step toward into simplicity and miniaturization based on lateral flow concepts, a technic widely used in immunological diagnostic in biological laboratories.

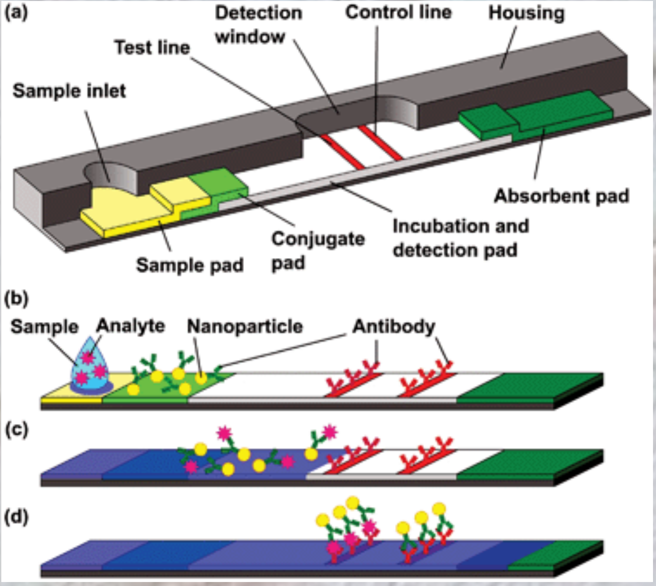

Mark. D. Microfluidic lab-on-a-chip platforms: requirements, characteristic and applications. Chem. Soc. Rev 39 (2010)

BUDGETS

Mass estimation: 8 Kg (including a 30% of margin)
Power estimation: 20 watts (peak)
Energy estimation: TBC watts/hour
Data estimation: TBC Mbytes

CONCLUSION

1. NASA lander design looks still quite immature (¿?).
2. Many design drivers are not defined.
3. AWL should be understand like one of the possible instruments that is in line with Europe Initiative goals.
4. Imaging system (¿?)

….. a classical awl


BACK UP

PROP-F (PHOBOS MISSION)

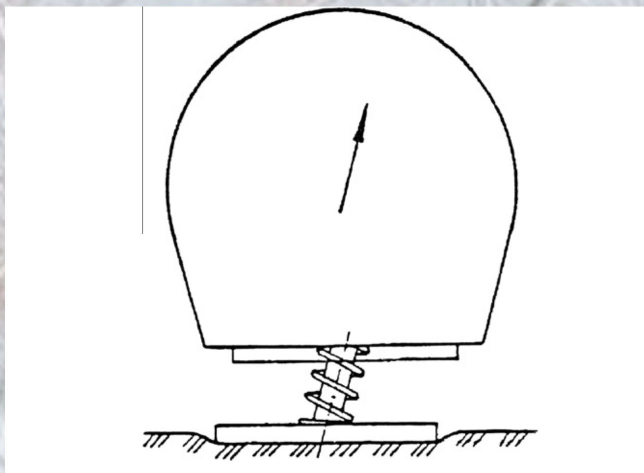

Fig. 3. Concept of PROP-F hopper (Kemurdzhian et al., 1988).

PROP-F was to be disconnected from the main spacecraft by means of a pyrotechnic device and then ejected with a preloaded spring at an altitude of approximately 1–2 km above the surface of Phobos. The energy stored in the separation spring was 6.2 ± 0.2 J. The velocity of the separation would have been 0.4–0.6 m/s vertically

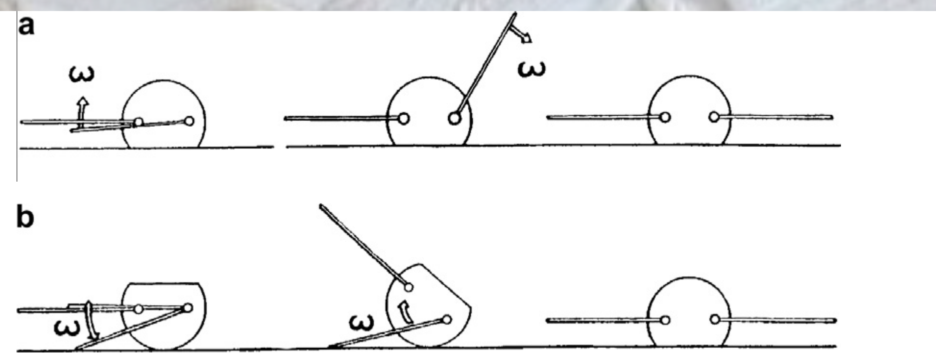

Fig. 4. Phobos Hopper re-orientation concept: (a) upside up and (b) upside down (Kemurdzhian et al., 1988).

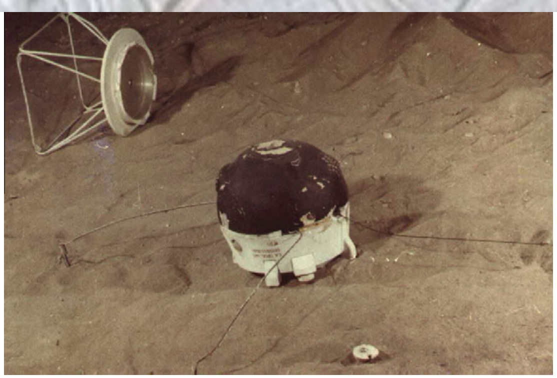

Fig. 5. Phobos Hopper qualification model after test (courtesy: VNIITransmash).

Ulamec et al. Hopper concepts for small body landers. Advances in Space Research 47 (2011) 428-439

MINERVA (HAYABUSA MISSION)

MIcro/Nano Experimental Robot Vehicle for Asteroid

The mass of Minerva was only 591 g. It was equipped with three CCD cameras (one single and one stereo pair), sun sensors and thermometers as payload. The robot had a diameter of 120 mm and would have hopped by means of an internal torquer (Yoshimitsu et al., 2003, 2006).

This torquer was designed to cause a reaction force against the surface of the asteroid, forcing the landed device to hop with a significant horizontal velocity. With the given DC motor, depending on the surface friction, a maximum hopping velocity of 10 cm/s was envisaged (Yoshimitsu et al., 2003).

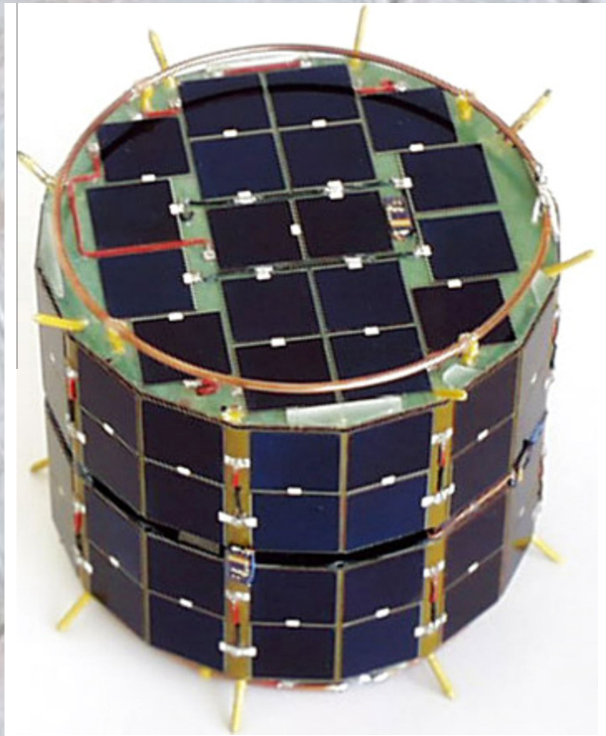

Fig. 7. Minerva hopper (image: JAXA).

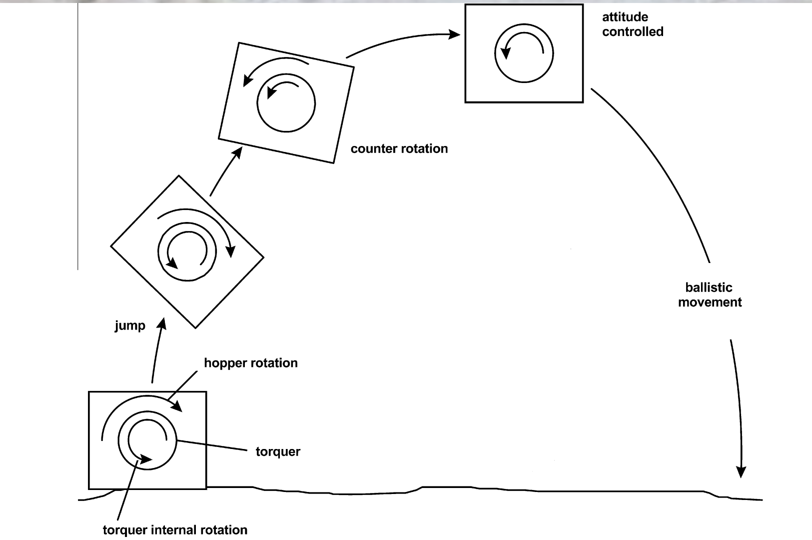

Fig. 6. Minerva mobility concept (from Kubota and Yoshimitsu (2007)).

Ulamec et al. Hopper concepts for small body landers.
Advances in Space Research 47 (2011) 428-439

MINERVA (HAYABUSA MISSION)

Table 1
Developed robot specifications

Body size	Octangle pole ϕ: 120 mm, height: 100 mm
Weight	550 g
Mobility system	Turn table to decide the direction
Power supply	Solar panels (peak power: 2.2 W, 1 AU) Condenser (2.3 V, 50 F) $\times$ 2
Onboard CPU	32 bit CPU
Communication	9600 bps (max range: 20 km)
Payload	CCD camera $\times$ 2 Sun sensor $\times$ 6 Thermometers
Power consumption	2.6 W for actuators (max.) 1.8 W for communication 1.8 W for camera 0.8 W for on-board computer
DC motor (hop)	No load speed: 11,400 rpm Stall torque: 8.80 mNm Torque constant: 3.96 mNm/A (measured in 4.8 V)

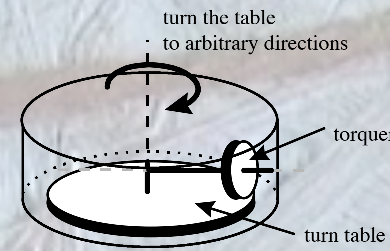

Fig. 2. Robot with turntable inside.

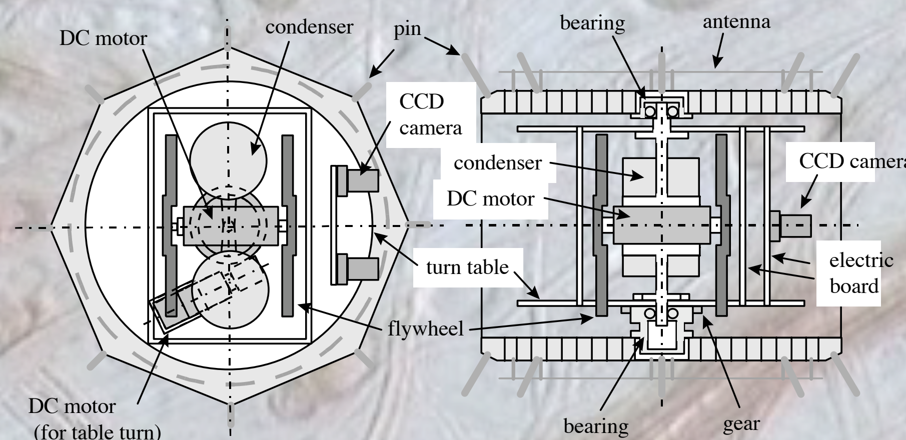

Fig. 4. Internal layout of developed robot.

Yoshimitsu et al. Micro-hopping robot for asteroid exploration.
Acta Astronautica 52 (2003) 441-446

MASCOT (HAYABUSA)

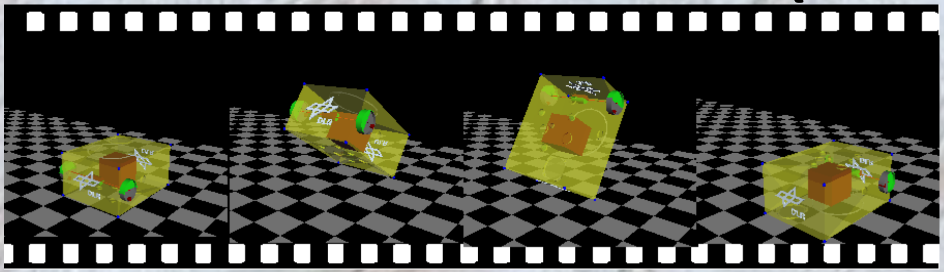

Fig. XXII: Upright sequence; turnaround (from left to right)

	Dry Mass [kg]	Eff. Margin %	Wet Mass [kg]
Structure	2.90	0.0	2.90
Thermal Control	0.41	15.4	0.47
Mechanisms	0.48	17.8	0.57
Communications	0.36	10.0	0.40
DHS	0.40	20.0	0.48
Power	1.00	12.0	1.12
Harness	0.30	20.0	0.36
Payload	3.00	0.0	3.00
Attitude Determination	0.20	20.0	0.24
Landed Mass	9.1		9.5
Interface Parts	1.5	13.0	1.7
Subtotal			11.3
Total incl. 20% System Margin			13.5

Table I: Mass breakdown table

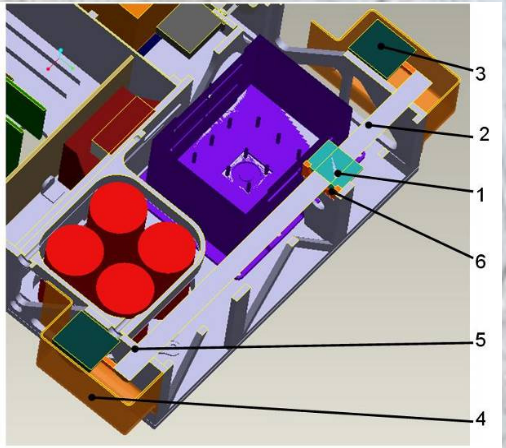

Fig. XXVII: Mobility System Components

Basically the mechanism consists of the motor-gear unit (1) and an axle (2), which transmits the torque to the inertia masses (3) on both sides of MASCOT. These masses are located outside the inner structure of MASCOT for package reasons, although they are protected by a cover (4). The transmission axle is mounted in sealed ball bearings (5). A mounting plate (6) supports the motor-gear unit to the MASCOT structure.

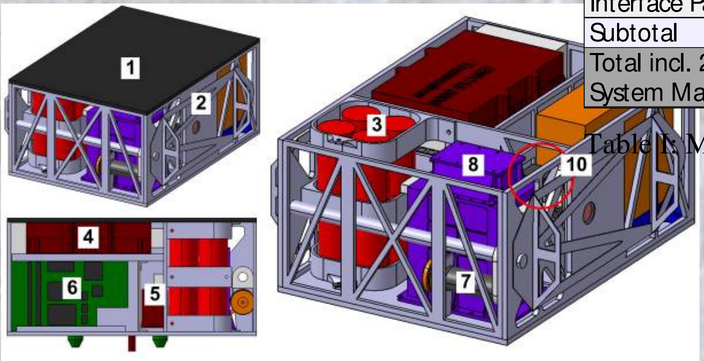

Fig. III: MASCOT configuration isometric and side view with (1) sandwich top plate, (2) main aluminium structure (3) battery pack, (4) transceiver unit and (5) Rx-filter, (6) common E-box, (7) motor and gear for the mobility mechanism, (8) MicroOmega, (9) ILMA, (10) Camera

Payload

- ILMA (Ion Trap Mass Spectrometer) or XRD/XRF or Bi-static radar of 2 kg
- VIS and Infrared Microscope of 0.7 kg
- Wide Angle Camera of 0.3 kg

Dietze et al. Landing and Mobility Concept for the Small Asteroid Lander Mascot on Asteroid 1999 JU3
61th Int'l Astronuatucai Congress, Prague (ACI-10.A3.5.8

WISKER CONCEPT

In the following we would like to describe one concept for a ~10 kg hopping surface package in more detail. The proposed design would be applicable, e.g. as payload for the Hayabusa 2 mission and could accommodate 2.5–3 kg of scientific payload. The slightly wedge shaped

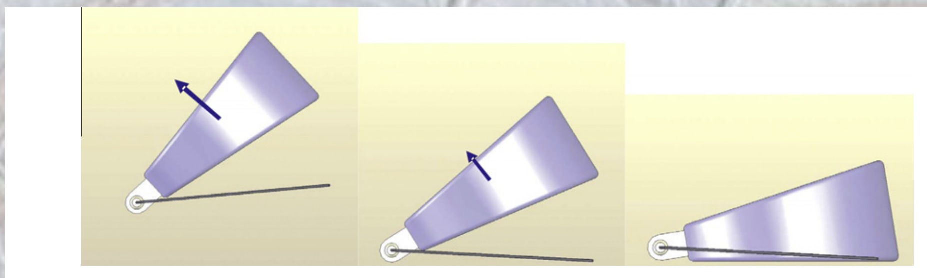

Fig. 9. Concept of hopping with whiskers.

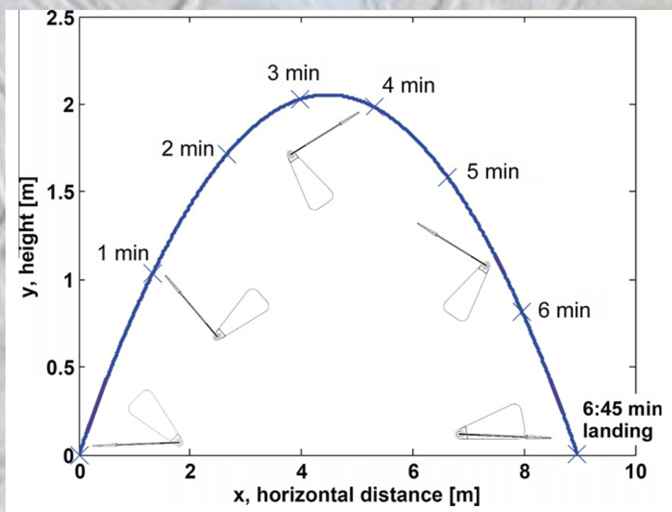

Fig. 17. Trajectory of a jump with an initial velocity of 3 cm/s in a 10^{-4} m/s^2 gravitational environment. The take-off angle in this example is 42.5°.

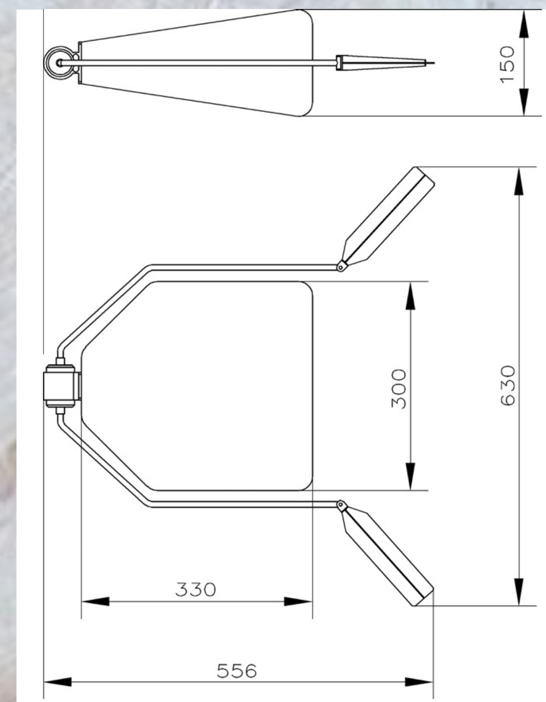

Fig. 12. Dimensions of analyzed hopper design (in mm).

Ulamec et al. Hopper concepts for small body landers.
Advances in Space Research 47 (2011) 428-439

CUBLI

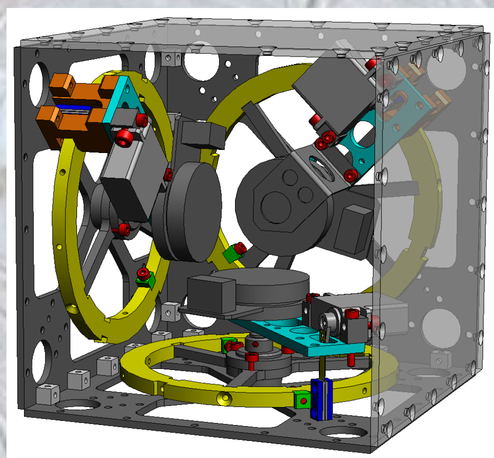

Fig. 3. The CAD drawing of the Cubli with one of the acrylic glass covers removed.

***Abstract*— The Cubli is a $15 \times 15 \times 15$ cm cube with reaction wheels mounted on three of its faces. By applying controlled torques to the reaction wheels the Cubli is able to balance on its corner or edge. This paper presents the development of the Cubli. First, the mechatronic design of the Cubli is presented. Then the multi-body system dynamics are derived. The parameters of the nonlinear system are identified using a frequency domain based approach while the Cubli is balancing on its edge with a nominal controller. Finally, the corner balancing using a linear feedback controller is presented along with experimental results.**

Gajamohan M. et al. The Cubli: a Reaction Wheel Based 3D Inverted Pendulum

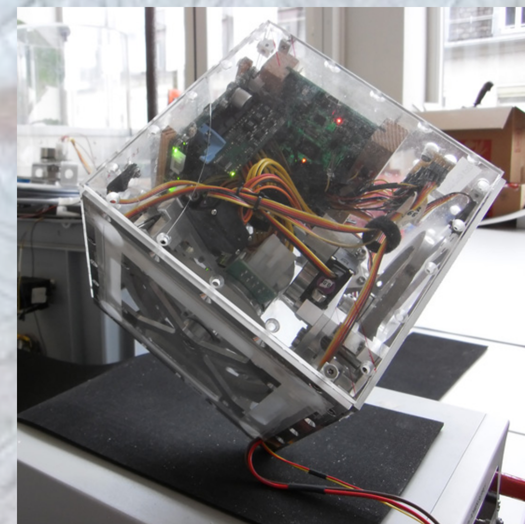

Fig. 1. Cubli balancing on the corner. In the current version, the Cubli (controller) must be started while holding the Cubli near the equilibrium position. Power is provided from an external constant voltage supply.

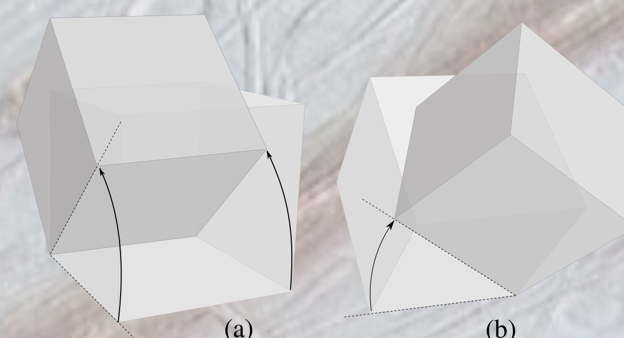

Fig. 2. The Cubli jump-up strategy: (a) Flat to Edge: Initially lying flat on its face, the Cubli jumps up to stand on its edge. (b) Edge to Corner: The Cubli goes from balancing on an edge to balancing on a corner.

MAGNETOMETER

TABLE I

The Background and the Primary Fields at Europa and Callisto before and during Encounters C3, C9, E4, and E14

Encounter		Field component[a]	From Galileo data: $\mathbf{B}_J$ at C/A (nT)[b]	From Galileo data: $\mathbf{B}_{prim,C/A}$ (nT)[c]	From Khurana (1997) model: $\mathbf{B}_{prim,C/A}$ (nT)[d]	From Khurana (1997) model, for times t during the 1/4 synodic period before C/A: Max. angle $(\mathbf{B}_{prim}(t), \mathbf{B}_{prim,C/A})$[e]	From Khurana (1997) model, for times t during the 1/4 synodic period before C/A: Max. (min.) of $B_{prim,C/A} - B_{prim}(t)$ (nT)[f]
Callisto	C3	B_x	−2.4	−2.4	−3.4		
		B_y	−31.7	−31.7	−33.4	5.5°	3.2 (−3.0)
		B_z	−10.8	0	−0.3		
	C9	B_x	1.7	1.7	5.8		
		B_y	33.65	33.65	33.9	8.6°	2.2 (−7.5)
		B_z	−10.7	0	−1.9		
Europa	E4	B_x	53.4	53.4	49.8		
		B_y	−176.2	−176.2	−172.0	148.5°	0 (−104.0)
		B_z	−410.0	0	−21.0		
	E14	B_x	9.6	9.6	10.1		
		B_y	−212.2	−212.2	−213.2	132.5°	0 (−138.1)
		B_z	−402.7	0	−17.6		

Note. This table lists values used in assessing the background field $\mathbf{B}_J$, the primary field at closest approach $\mathbf{B}_{prim,C/A}$, and the temporal variation of the primary field $\mathbf{B}_{prim}(t)$ before each of the considered encounters. For the construction of the model fields of Figs. 3–6, $\mathbf{B}_j$ and $\mathbf{B}_{prim,C/A}$ were estimated using *Galileo* data (see Sections 4.1.1 and 4.2). For the analysis of the phase lag (Sections 4.1.2 and 4.2.2), $\mathbf{B}_{prim,C/A}$ and $\mathbf{B}_{prim}(t)$ were determined from the Khurana (1997) model ($\mathbf{B}_{prim}(t) = \langle \mathbf{B}_J \rangle - \mathbf{B}_J(t)$, where $\mathbf{B}_J(t)$ is the model jovian background field predicted at the moon's position at time t and the brackets denote an average over many synodic periods).

[a] All field components are given in the moon-centered coordinate systems defined in Section 4.1.1 for Callisto and 4.2 for Europa.

[b] Jovian background field at the location of the moon at the time of closest approach,. estimated from *Galileo* measurements (see Section 4.1.1).

[c] Primary field at closest approach, estimated from the equatorial projection of the background field at closest approach given by the previous column.

[d] Primary field at closest approach, estimated from the Khurana (1997) model. Note that it does not differ appreciably from the primary field estimated using *Galileo* data given in the previous column. In particular, the component B_z is small compared to B_x and B_y, as expected (see Section 2).

[e] Largest angular separation between the primary field at closest approach and the primary field during the preceding 1/4 synodic period.

[f] Largest (smallest) algebraic difference between the magnitude of the primary field at closest approach and the magnitude of the primary field during the preceding 1/4 synodic period.

Zimmer et al. Subsurface Oceans on Europa and Callisto: Constrains from Galileo Magnetometer Observations. Icarus (2000) 147

MAGNETOMETER

http://www.cubesatshop.com/product/nss-magnetometer/

Orthogonality: better than +/- 1°
Measurement range: +60,000nT to -60,000nT
Sensitivity: 6.5nT
Update rate: up to 10Hz
Noise density: <500pT RMS/Hz @1Hz
Power consumption: <700 mW
3-axis analogue output: 0-5V or Serial (RS422 or I2C)
Temperature output 0-5V
Dimensions: 96x43x17mm
Mass: <200g
Operating temperature: -35°C to +75°C
15g rms random vibration (qualification levels)
10krad total dose (component level)

MAGNETOMETER

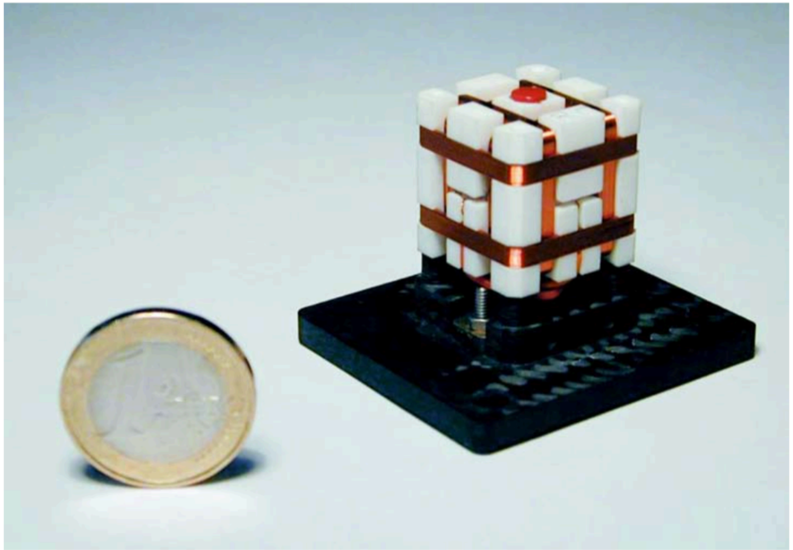

Figure 2. The RPC-MAG fluxgate sensor.

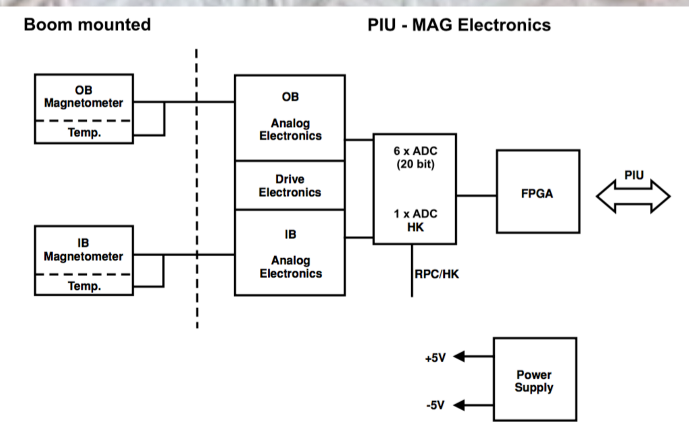

Figure 4. The RPC-MAG block diagram. The sensors are boom mounted and connected to the Plasma Interface Unit (PIU) via the sensor analog electronics.

ROSETTA RPC-MAG orbiter

RPC-MAG requirements

Range ±16384 nT
Quantization 20 bit; 31 pT
Sampling rate 20 vectors/s
Bandwidth 0–10 Hz

Dimensions: 25x25x25 mm^3
Mass of 28g

Ref. Galssmeier et al. The Fluxgate Magnetometer in the ROSETTA Plasma Consortium. Space Science Review (2007) 128

ICE DRILLING

Several techniques have been proposed in the past:

Fig. 1. A photographic view of the USDC held from its cable while coring sandstone. The minimal need for axial force is easily seen.

Ultrasonic core driller

Bar-Cohen Y, et all, Ultrasonic/Sonic Driller/Corer (USDC) as a Sampler for Planetary Exploration. 2001. IEEE Aerospace Conf.

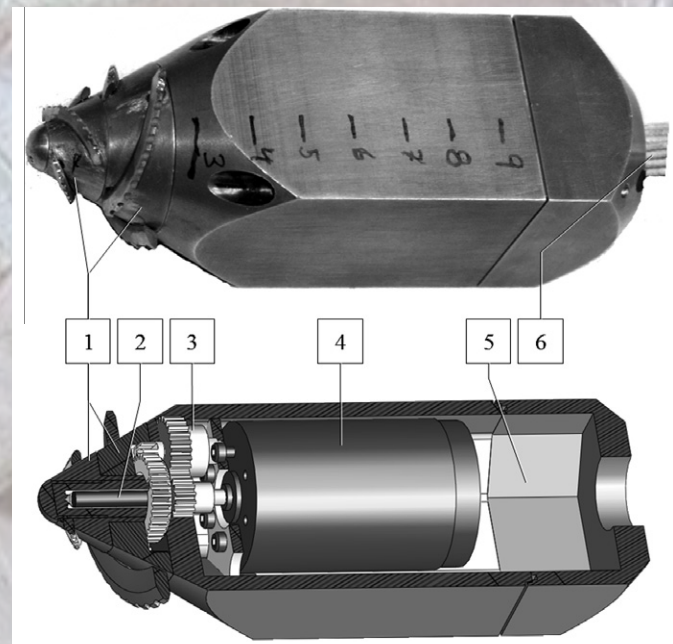

Fig. 1. The thermal drill prototype and its internal components: [1] rotary blades, [2] cartridge heater (four others in the corners are not shown), [3] gear, [4] motor, [5] tether compartment and [6] cable.

Thermal drill

Weiss et al. Thermal drill sampling system onboard high velocity impactors fo exploring the subsurface of Europa. Advance in Space Research (2011),48

Fig. 3. Ice block penetrated by CO_2 laser irradiation. The laser entered fron picture. The hole diameter is about 4 mm and the hole length is about 13 c is under the ice block in the front.

Laser drill

Sakurai et al, Studies of melting ice using CO2 laser for ice drilling. Cold Regions Science and Technology (2015)